

# Series-Type Switched-Inductor Z-Source Inverter

Xupeng Fang, Yingying Tian, Xiaokang Ding, and Bolong Ma

**Abstract**—To solve the disadvantages of the traditional Z-source inverter (ZSI), this paper investigates a series-type switched-inductor Z-source inverter (SSI-ZSI) topology. It not only preserves the advantages of the traditional ZSI, but also improves the voltage gain. On the condition of the same voltage gain, the capacitor voltage stress is reduced, the soft start characteristic can be achieved and the inverter can be immune to the damage of the inrush current. The circuit structure and operating principle are analyzed in detail; the simulation model and the experimental platform are built. The simulation and experimental results verify the rationality and superiority of the circuit topology.

**Index Terms**—Switched-inductor, ZSI, PWM, series-type.

## I. INTRODUCTION

IN recent years, with the increasing consumption of the major traditional energy sources such as oil, coal and natural gas and the increasing emphasis on the environmental protection, the development and utilization of green and clean energy sources has received increasing attention [1]-[2]. However, the most output of the new energy power is unsteady DC power; the DC/AC converter is required and is a very crucial link in the power conversion [3]. At present, the voltage source inverter is widely used in the low and medium power level green energy power generation applications. But it is a buck converter; a boost converter is often inserted before the inverter bridge to obtain a wide range output ac voltage, but this two stage power conversion scheme will lead to low power conversion efficiency, bulky circuit structure, high system cost. And in order to avoid the shoot-through issue of the same bridge leg turning on simultaneously, it is necessary to add dead time in the control signal of the same bridge leg power switches to strengthen the reliability of the system, which will lead to the quality deterioration of the output waveform [4]-[6]. There are many modified topologies and control strategies to deal with the above problems, but they all have more or less limitations and problems and could not satisfy the requirements of the practical applications.

Under this background, the ZSI topology is proposed in 2002 by Professor Peng Fang zheng to solve the above problems of the traditional voltage source inverter-based new energy power generation system [6], it mainly aims to the fuel cell power generation application whose input DC voltage varies in a very

wide range, the novel inverter topology uses a unique symmetry Z-source network to allow the two power switches of the same bridge leg turning on at the same time to realize the buck-boost function. Due to the existence of the shoot-through state, the dead time needs not to be added like the conventional inverter, so the reliability of the inverter and the quality of the output waveform can be improved. However, the ZSI also has inherent deficiencies, such as limited boost ability, large capacitor voltage stress and inrush current during startup, which easily damages the inverter device, shortens the lifetime of the inverter and increases the complexity of the circuit. A quasi-Z-source inverter (Q-ZSI) topology is proposed in [7] to solve the shortcomings of the ZSI that discontinuous input current and large capacitor voltage stress, which are derived from the ZSI circuit structure, only the position of the impedance-source network components is slightly changed, without adding additional components, its DC source and the inverter bridge have common node, thus simplifies the circuit structure. The improved Z-source inverter (I-ZSI) topology is designed in [8] to solve the problems of large capacitor voltage stress and serious loop impact at power-on of the impedance-source network. Because the ZSI is just reversed, choosing the appropriate control strategy can suppress the impact of the starting voltage and current and achieve a soft start function to avoid damage to the inverter. A switched-inductor Z-source inverter (SI-ZSI) topology is presented in [9] to improve the boosting ability. Although this topology can greatly increase the boost capability, the capacitor voltage stress is still large and increases the capacitor size and cost.

Two novel topologies that named  $\Delta$ -source inverter and Y-source inverter have been proposed in recent years.  $\Delta$ -source inverter has two degrees of freedom that can be adjusted to achieve high voltage gain. It can be changed either by changing the value of the shoot-through duty ratio ( $D$ ) or by changing the winding factor. But, this topology has some disadvantages, such as the leakage inductance of the coupled three inductors will affect the operation of the inverter, which leads to large circuit losses and low inverter efficiency. Y-source inverter has a Y-shaped three-winding coupled inductor network to form a pre-stage boost circuit. However, its output voltage is very sensitive to leakage inductance of the coupled inductors. In practice, precise closed-loop control is required, which makes the circuit cost increase and the control is complicated.

In view of the disadvantages of the traditional ZSI and its series modified topologies, combined with the advantages of the topology proposed in [8] and [9], this paper proposes an improved switched-inductor inverter topology, that is, the

Manuscript was submitted for review on 27, November, 2018.

Xupeng Fang, Yingying Tian, Xiaokang Ding, and Bolong Ma are with College of Electrical Engineering and Automation, Shandong University of Science and Technology (e-mail: skdfxp@163.com; 297764648@qq.com; 1091272417@qq.com; 1570630609@qq.com)

Digital Object Identifier 10.30941/CESTEMS.2020.00008

series-type switched inductor Z-source inverter (SSI-ZSI). The topology maintains high boost capability characteristic, the capacitor voltage polarity is consistent with the input voltage, and its voltage stress is greatly reduced. In addition, there is no current path at startup, which solves the drawback of the ZSI, eliminates the startup inrush current, and can achieve soft start.

## II. TOPOLOGY AND OPERATING PRINCIPLE ANALYSIS

The circuit structure of SSI-ZSI is shown in Fig. 1. It is derived from the I-ZSI, that is, the three-phase inverter bridge and the input side diode  $D_0$  are exchanged, the inductors  $L_1$  and  $L_2$  are replaced by the two boosting units, each boosting unit is composed of two switched inductors, that is, replacing the original  $L_1$  with the boosting unit 1 consisting of  $L_1, L_2, D_1, D_2,$  and  $D_5$ , and replacing the original  $L_2$  with a boosting unit 2 consisting of  $L_3, L_4, D_3, D_4,$  and  $D_6$ . It not only retains the advantages of the I-ZSI that has lower capacitor voltage stress, continuous input current and less inrush current, but also retains the advantages of the SI-ZSI which has high boost ability.

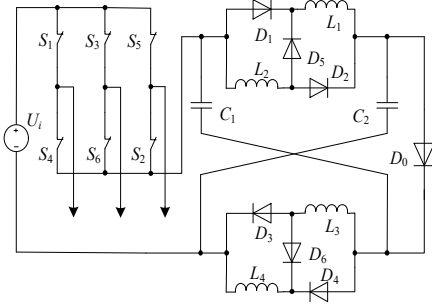
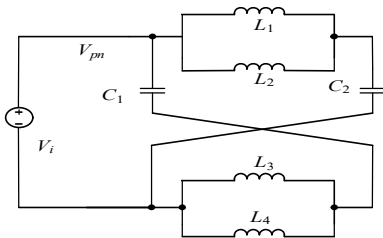


Fig. 1 The topology of SSI-ZSI.

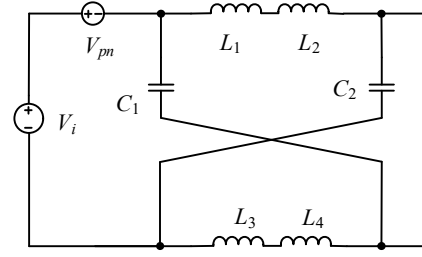
Same to the ZSI, the SSI-ZSI can also realize buck/boost function by the inserting of the shoot-through zero states. To simplify the circuit analysis process, let  $L_1 = L_2 = L_3 = L_4 = L$ ,  $C_1 = C_2 = C$ .

In the shoot-through zero state, the diodes  $D_1, D_2, D_3,$  and  $D_4$  are all forward biased and turned on. The diodes  $D_0, D_5,$  and  $D_6$  are all reverse biased and turned off. The inductors  $L_1, L_2$  are connected in parallel and  $L_3, L_4$  are connected in parallel in the two boost units. They are charged by the capacitors  $C_1, C_2,$  respectively. The equivalent circuit of the inverter is shown in Fig. 2(a).

In the non-shoot-through state, the diodes  $D_1, D_2, D_3,$  and  $D_4$  are all reverse biased and turned off simultaneously, the diodes  $D_0, D_5,$  and  $D_6$  are all forward biased and simultaneously turned on. The inductors  $L_1, L_2$  in series, and  $L_3, L_4$  in series in the two boost units, and they supply the capacitors  $C_1, C_2$  and the load, respectively. The equivalent circuit of the inverter is shown in Fig. 2(b).



(a) Shoot-through zero state



(b) Non-shoot-through state

Fig. 2. The equivalent circuit of the SSI-ZSI.

From the symmetry of the new Z-source network, the following formula is available

$$\begin{cases} V_{L1} = V_{L2} = V_{L3} = V_{L4} = V_L \\ V_{C1} = V_{C2} = V_C \end{cases} \quad (1)$$

When the inverter operates in the shoot-through zero state, as shown in Fig. 2 (a), there are

$$V_L = V_i + V_{C1} \quad (2)$$

$$V_{pn} = 0 \quad (3)$$

When the inverter operates in the non-shoot-through state, as shown in Fig. 2 (b), there are

$$V_{pn} = V_i + 2V_C \quad (4)$$

$$4V_L + V_{pn} - V_i = 0 \quad (5)$$

From (4) and (5), we have

$$V_L = -\frac{1}{2}V_C \quad (6)$$

According to the volt-second balance principle of the inductor, one has

$$DT(V_i + V_C)L_L + (1-D)T(-\frac{1}{2}V_C)L_L = 0 \quad (7)$$

Then we can have

$$V_C = \frac{2D}{1-3D}V_i \quad (8)$$

From (4) and (8), we have:

$$V_{pn} = \frac{1+D}{1-3D}V_i \quad (9)$$

The boost factor  $B$  is:

$$B = \frac{V_{pn}}{V_i} = \frac{1+D}{1-3D} \quad (10)$$

The output phase voltage  $V_o$  is:

$$V_o = M \frac{V_{pn}}{2} = MB \cdot \frac{V_i}{2} \quad (11)$$

Bringing (10) into (11), one has

$$V_o = \frac{M}{2} \cdot \frac{1+D}{1-3D} V_i \quad (12)$$

The voltage gain ( $G$ ) can be obtained:

$$G = \frac{V_o}{V_i/2} = MB = M \cdot \frac{1+D}{1-3D} \quad (13)$$

According to (11), the output phase voltage of the SSI-ZSI is not only related to the modulation index ( $M$ ), it but also related to the boost index ( $B$ ). Adjusting both of them can also achieve the buck-boost function.

### III. COMPARISON OF THE CHARACTERISTICS OF THE FOUR RELATED TOPOLOGIES

The boost capability of the SSI-ZSI is compared with other three related inverters, the relationship between  $B$  and  $D$  of the above four topologies is shown in Fig. 3.

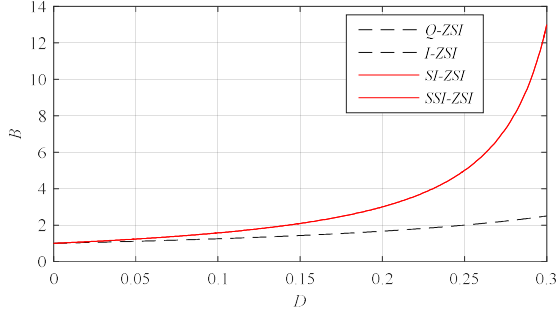


Fig. 3. The boost ability of the four related topologies.

From the Fig. 3, the SSI-ZSI and SI-ZSI have the same and strongest boost ability; the I-ZSI and Q-ZSI have the same and weaker boost ability. When the input voltage is constant, the DC-link voltage increases as  $D$  increases. When  $M$  and  $D$  are mutually constrained and the ideal boost factor cannot be realized, the SSI-ZSI topology can be used to achieve the required boost effect. If  $D$  is low,  $M$  can be increased as much as possible to maximize the DC-link voltage conversion efficiency and optimize the output voltage [10].

The relationship between the capacitor voltage stress  $V_C/V_i$  and  $D$  of the four topologies is shown in Fig. 4. With the same  $D$ , the capacitor voltage stress of SI-ZSI is the largest and that of the I-ZSI is the smallest. The capacitor voltage stress of SSI-ZSI is much lower than that of SI-ZSI, which is derived from the combination of these two topologies, especially when  $D < 0.227$ , which is smaller than Q-ZSI. Because the SSI-ZSI has high boost ability,  $D < 0.2$  is generally set, which can make the capacitor voltage stress at a small value to decrease the circuit size and cost.

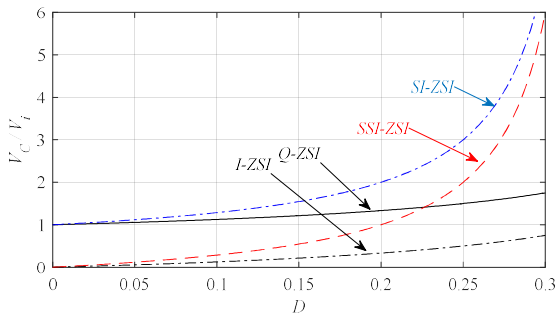


Fig. 4. The capacitor voltage stress of the four topologies.

When the four Z-source topologies aforementioned adopt the simple boost control strategy,  $M$  maximally is  $M=1-D$  and the voltage stress of the switch is the largest [11]. There are

$$G = MB = \frac{2M - M^2}{3M - 2} \quad (14)$$

The switch voltage stress:

$$\frac{V_S}{V_i} = \frac{V_{pn}}{V_i} = \frac{G}{M} \quad (15)$$

From (14) and (15):

$$\frac{V_S}{V_i} = \frac{2G}{2 - 3G + \sqrt{9G^2 - 4G + 4}} \quad (16)$$

The relationship between the power switch voltage stress  $V_S/V_i$  and the voltage gain  $G$  of the four circuit topologies aforementioned is shown in Fig. 5. Under the same  $G$ , the switch voltage stress of the Q-ZSI and I-ZSI are the same and larger, and that of the SI-ZSI and SSI-ZSI are the same and smaller. As  $G$  increases, this advantage of SI-ZSI and SSI-ZSI is more prominent. In addition, assuming that the four inverters have the same switch voltage stress, the SSI-ZSI and SI-ZSI can obtain higher voltage gain [12].

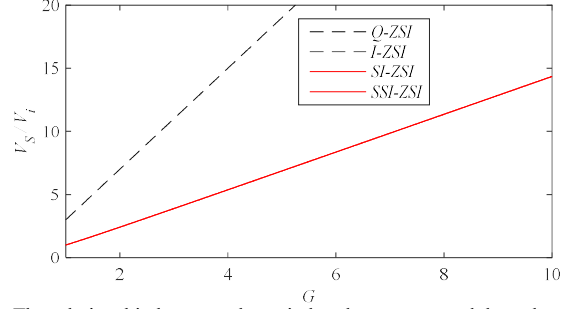


Fig. 5. The relationship between the switch voltage stress and the voltage gain.

### IV. THE CONTROL STRATEGY OF THE INVERTER

Due to the traditional zero vector and the shoot-through zero vector have the same effect on the SSI-ZSI, which both short-circuit the three-phase load and the inverter bridge. Therefore, in one switch cycle, the partial zero vectors can be directly replaced by the shoot-through zero vectors, which can achieve the simple boost control method of the SSI-ZSI conveniently, as shown in Fig. 6. Choosing voltages  $V_n$  and  $V_p$  whose value are between the sinusoidal modulated wave and the triangular carrier. If the instantaneous value of the triangular carrier is larger than  $V_p$  or less than  $V_n$ , the SSI-ZSI operates in the shoot-through state; otherwise, the SSI-ZSI operates in the traditional SPWM modulation state [13]-[15].

In the non-shoot-through state,  $G$  of the SSI-ZSI is determined by the product of  $B$  and  $M$ . When  $G$  is large,  $B$  should be reduced and  $M$  be increased as much as possible to reduce the switching voltage stress.  $V_n, V_p$  should satisfy:

$$\begin{cases} V_n \leq (1-M)V_Z \\ V_p \geq (M-1)V_Z \end{cases} \quad (17)$$

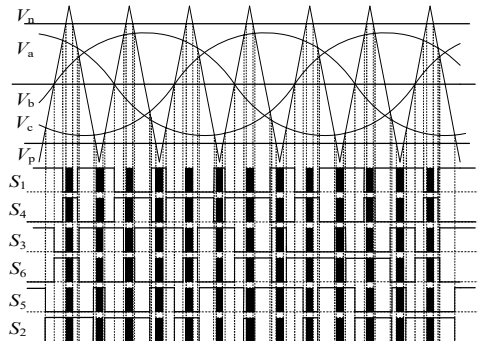


Fig. 6. Schematic diagram of the simple boost SPWM control method.

Where  $V_Z$  is the peak value of the carrier voltage.

In the simple boost control method, when  $M$  is increased,  $D$

is reduced, and  $D$  cannot be larger than  $(1-M)$ . Therefore, when  $M$  is 1, the maximum  $D$  is 0.

According to (14), the relationship between  $G$  and  $M$  can be obtained and as shown in Fig. 7. From Fig. 7, the right side of the curve, the SSI-ZSI operates in the simple boost control mode,  $G$  decreases as  $M$  increases, and when  $M$  is equal to 1,  $G$  is equal to 1, that is, the SSI-ZSI has no boost ability in this case. To get a larger  $G$ ,  $M$  must be lowered, but in this situation, it will lead to the output waveform quality of the inverter worsen, and the switch voltage stress increase.

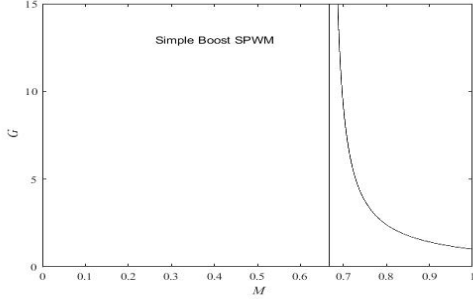


Fig. 7. The relationship between  $G$  and  $M$ .

According to (16), the relationship between the power switch voltage stress  $V_s/V_i$  and  $G$  are redrawn in Fig. 8. From Fig. 8, in the simple boost SPWM control mode, the  $V_s/V_i$  increases as  $G$  increases and is much larger than  $G$ .

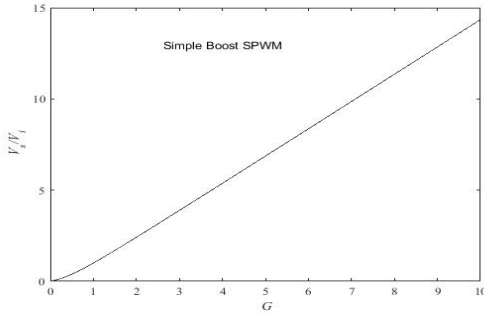


Fig. 8. The relationship between  $G$  and  $V_s/V_i$ .

## V. THE SWITCHING LOSS OF THREE-PHASE SHOOT-THROUGH MODE

As we known, ZSIs have single-phase, two-phase and three-phase shoot-through modes. The simple boost SPWM control strategy is applied in the three-phase shoot-through control mode. Although it will increase the switching times, this method is relatively easy, so it is widely used in ZSIs [14]. The equivalent circuit of the inverter bridge when operates in the three-phase shoot-through mode is shown in Fig. 9.

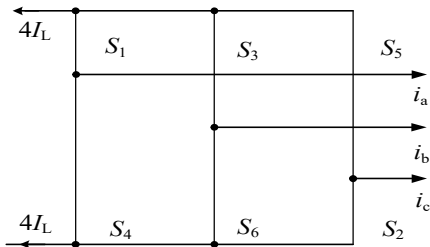


Fig. 9. The equivalent circuit of three-phase shoot-through state.

According to KCL, from Fig. 9, we can have

$$\begin{cases} i_{S1} = i_{S4} + i_a \\ i_{S3} = i_{S6} + i_b \\ i_{S5} = i_{S2} + i_c \\ i_{S1} + i_{S4} = i_{S3} + i_{S6} = i_{S5} + i_{S2} \\ i_{S1} + i_{S3} + i_{S5} = i_{S4} + i_{S6} + i_{S2} = 4I_L \\ i_a + i_b + i_c = 0 \end{cases} \quad (18)$$

Then

$$\begin{cases} i_{S1} = \frac{4}{3}I_L + \frac{1}{2}i_a \\ i_{S2} = \frac{4}{3}I_L - \frac{1}{2}i_c \\ i_{S3} = \frac{4}{3}I_L + \frac{1}{2}i_b \\ i_{S4} = \frac{4}{3}I_L - \frac{1}{2}i_a \\ i_{S5} = \frac{4}{3}I_L + \frac{1}{2}i_c \\ i_{S6} = \frac{4}{3}I_L - \frac{1}{2}i_b \end{cases} \quad (19)$$

The maximum current of the power switch is

$$I_{smax} = \frac{4}{3}I_L + \frac{1}{2}I_o \quad (20)$$

The maximum shoot-through loss of the power switch is:

$$P_3 = \left(\frac{4}{3}I_L + \frac{1}{2}I_o\right)^2 R \quad (21)$$

Due to the balance of the input and output active power of the inverter

$$V_i I_L = \sqrt{3}V_o I_o \cos \theta \quad (22)$$

Hence

$$I_L = \frac{\sqrt{3}V_o I_o \cos \theta}{V_i} \quad (23)$$

Similarly, the switching loss of single-phase shoot-through and two-phase shoot-through can be derived as

$$P_1 = \left(4I_L + \frac{\sqrt{3}}{2}I_o\right)^2 R \quad (24)$$

$$P_2 = \left(2I_L + \frac{\sqrt{3}}{8}I_o\right)^2 R \quad (25)$$

Where,  $I_L$  is the inductor current in the boost unit, and  $R$  is the internal resistance of the power switch.

Next, to the switching loss of the power diodes, according to the operating principle of the circuit, as aforementioned in part II, in the shoot-through zero state, the diodes  $D_1, D_2, D_3,$  and  $D_4$  are all forward biased and turned on. The diodes  $D_0, D_5,$  and  $D_6$  are all reverse biased and turned off. In the non-shoot-through state, the diodes  $D_1, D_2, D_3,$  and  $D_4$  are all reverse biased and turned off simultaneously, the diodes  $D_0, D_5,$  and  $D_6$  are all forward biased and simultaneously turned on. Since the reverse leakage current of the power diode is very small and can be neglected, it is reasonable to concern the power loss of the power diode in the turn on state.

Thus, the power loss of diodes  $D_1, D_2, D_3,$  and  $D_4$  can be

described as following,

$$P_D = I_L \cdot V_{on} \quad (26)$$

And if we neglect the variation of the Z-source network capacitor current, the power loss of diodes  $D_0$ ,  $D_5$  and  $D_6$  can be described as following,

$$P_D = I_L \cdot V_{on} \quad (27)$$

Where  $V_{on}$  is the voltage drop of the power diode in the on state.

### VI. SIMULATION AND EXPERIMENTAL RESULTS

The simulation model of the SSI-ZSI based on SPWM is built by Matlab/Simulink software. Fig.10 shows the upper and lower switch signals of one bridge leg. The simulation parameters are as follows: the DC input voltage  $V_i=24V$ ,  $D=0.18$ , the inductors of the boost unit  $L_1=L_2=L_3=L_4=2mH$ , capacitors of the new Z-source inverter  $C_1=C_2=1000\mu F$ , the three-phase load  $R=20\Omega$ , the switching frequency  $f_s=20kHz$ , the filter inductor  $L_f=5mH$ , the filter capacitor  $C_f=22\mu F$ , the modulation index  $M=0.8$ , the simulation waveforms are shown in Fig. 11.

As can be seen in Fig. 10, the inverter is in a steady state and the shoot-through zero vector has been added to the conventional zero vector. From Fig. 11, the data measured by the oscilloscope is: the capacitor voltage is 17.68V; the inverter bridge DC side voltage is 60.15V, the output AC line voltage peak value is 42.15V. The corresponding theoretical values are 18.78V, 61.56V, 42.60V, respectively. Comparing the simulation results with the theoretical values, it can be clearly concluded that the simulation results are consistent with the theoretical analysis.

To verify the dynamic performance of the SSI-ZSI system, the output AC waveform when the load is doubled at 0.15 seconds is shown in Fig. 12. It can be seen that the output voltage and current are stabilized after oscillation and the response time is very short, the output voltage can be stabilized at around 42V, and the output current is increased from 1.2 A to 2.4A. It is verified that the system has a fast closed-loop adjustment characteristic, that is, the sudden change of load has less influence on the output waveform of the inverter. This shows that the feedback loop designed in this paper based on simple boost SPWM control has strong anti-interference ability.

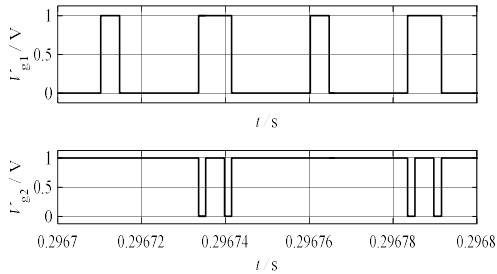


Fig. 10. The upper and lower switch signals of one bridge leg.

To further verify the rationality of the theoretical analysis of the SSI-ZSI and the correctness of the simulation results, the prototype has been constructed, which is shown in Fig. 16. The control module uses DSP TMS320F28335 for generating

signals based on simple boost SPWM modulation to control the switches.

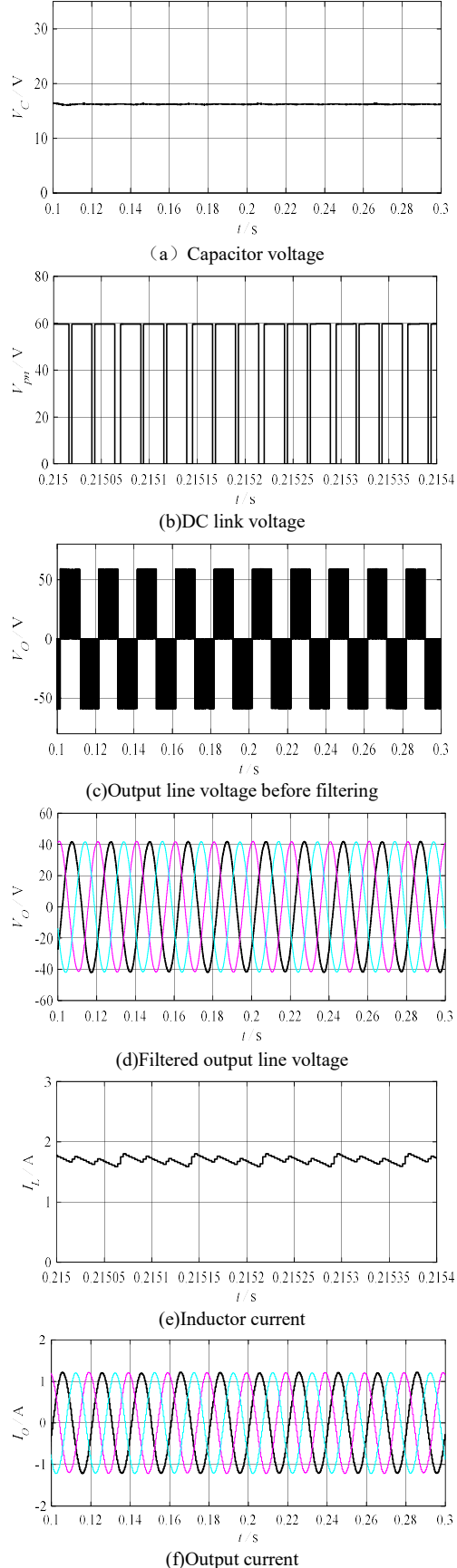


Fig. 11. Simulation waveforms based on SPWM control mode.

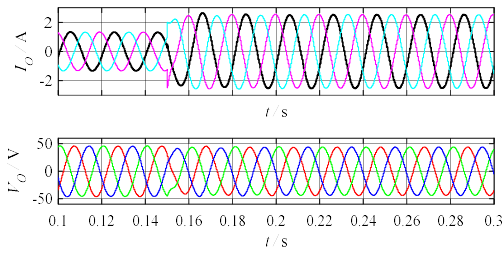


Fig. 12. The dynamic waveforms of the output voltage and current.

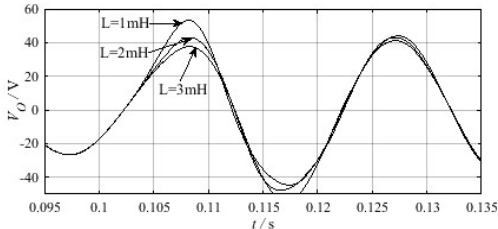


Fig. 13. When the inductance changes.

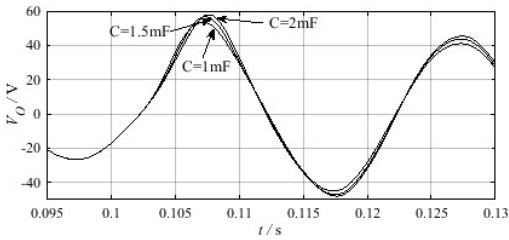


Fig. 14. When the capacitance changes.

Different parameters in the Z-source network will affect the system response speed and stability. In analyzing the dynamic characteristics of the SSI-ZSI network, in order to compare the effects of different network parameters on the output AC voltage in detail, the inverters are simulated with three different network parameters.

From Fig. 13, as the value of the inductor increases, the oscillation amplitude of the output voltage decreases, and the time for the system to rise, adjust, and stabilize becomes longer. From Fig. 14, as the capacitance value increases, the oscillation amplitude of the output voltage of the inverter increases, and the time for the system to rise, adjust, and stabilize tends to become longer. Therefore, when selecting the inductance and capacitance parameters, try to select the energy storage components with smaller capacity in system boost characteristics are satisfied. Moreover, the inverter can realize the soft start function of the capacitor voltage in Fig. 15.

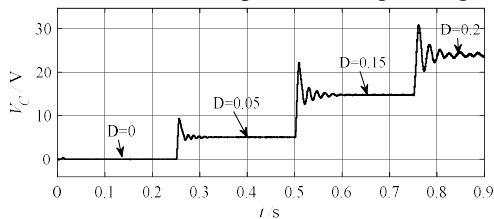


Fig. 15. Capacitor voltage waveform at soft start.

In the case that the experimental parameters are consistent with the simulation parameters, some experiments of the SSI-ZSI under simple boost SPWM control strategy are performed, and the waveforms of simple SPWM modulated signal before and after driving are shown in Fig. 17. The driven signal voltage is nearly 18V, and the IGBT selected can be driven and turned on and off normally.



Fig. 16. Experimental circuit.

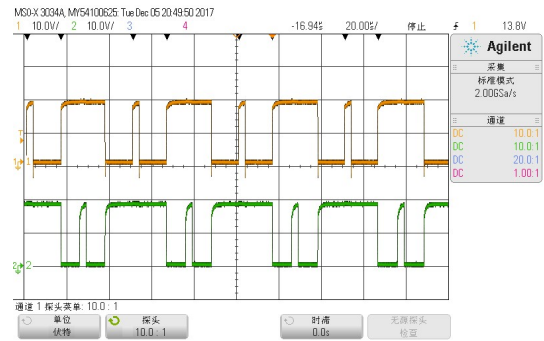


Fig. 17. The Driven signal of one bridge leg switches.

Fig. 19 shows the DC link voltage waveform of the SSI-ZSI. In the non-shoot-through state, the DC link voltage is about 60V, which is close to the theoretical value of 61.56V; when the inverter operates in the shoot-through zero state, the DC link voltage is zero, and the voltage of  $V_{pn}$  appears in PWM waveform in one cycle.

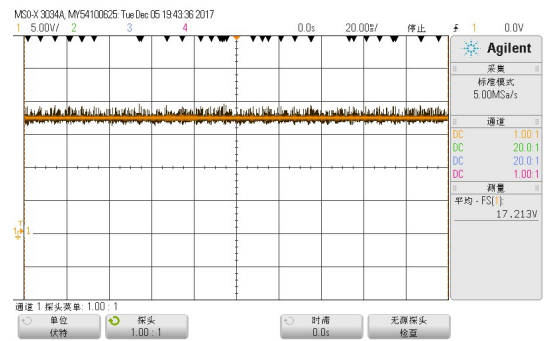


Fig. 18. Voltage of capacitor  $C_1$ .



Fig. 19. DC link voltage waveform.

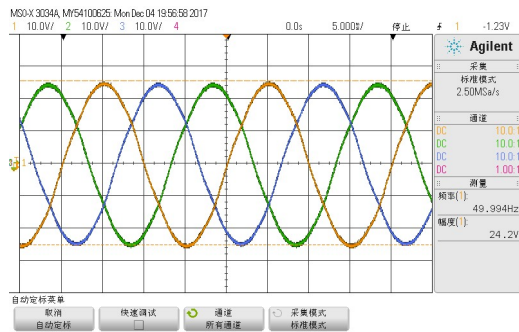


Fig. 20. Output phase voltage.

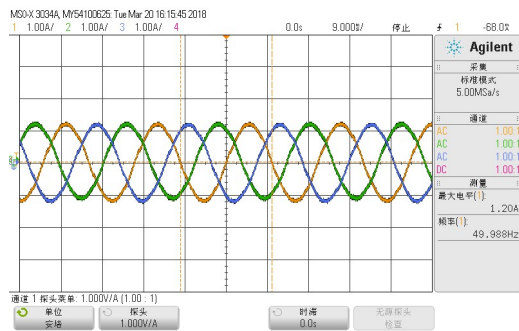


Fig. 21. Output phase current.

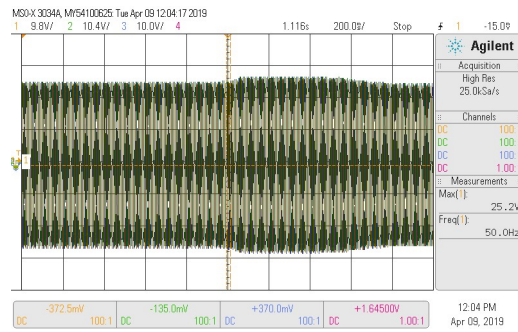
Fig. 20 is the output AC phase voltage waveforms of the inverter. The peak value of the voltage measured by the oscilloscope is 24.2V, and the theoretical value is 24.6V. Fig. 21 shows the output current waveform. The current amplitude measured is 1.2A, and the theoretical value is 1.23A. The experimental results are very close to the theoretical values, and the experimental waveforms are smooth sine waves. Fig. 22 shows the output AC phase voltage when the load changes and the shoot-through duty ratio  $D$  changes, where  $D$  is changed from 0.18 to 0.25. It indicates that when the load varies, the output AC phase voltage can keep stable, and when the shoot-through duty ratio  $D$  varies, the output AC phase voltage will varies correspondingly, and this also verifies the correctness of the theoretical analysis and the feasibility and reliability of the experimental prototype.

## VII. CONCLUSIONS

This paper presents a SSI-ZSI topology to solve the limitations of the conventional ZSI. The simulation model and experimental platform are built to simulate and verify its operating characteristics. Compared with the traditional ZSI, it has the following advantages:

- (1) It has a larger boost factor in the case of same shoot-through duty cycle  $D$ ;
- (2) In the case of same boost factor  $B$ , the capacitor voltage stress of impedance-source network can be greatly reduced;
- (3) It can dispense with the starting current check circuit, suppress the impact of the inrush current.

As a widely used power converter topology, it can be used not only in the DC-AC field, but also in the AC-AC, DC-DC and AC-DC fields. This paper only studies the one-way flow of energy. Considering the practical application, the inverter often needs to realize the two-way flow of energy. This paper does



(a) When the load changes

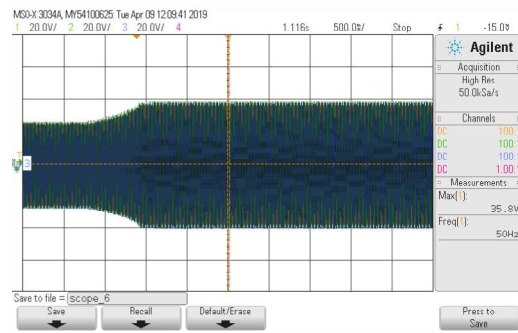
(b) When  $D$  changes

Fig. 22. Output AC phase voltage.

not study this, so we will study the directionality of energy flow in depth. In view of the limitations of experimental conditions and safety considerations, the experimental part of this paper only carries out experimental verification under the condition of low power, and needs to be verified at a higher power in the future.

## REFERENCES

- [1] Q. Gao, M. Qian, B., et al. "Analysis of an abnormal operating state of Z-source inverter". *Transactions of China Electrotechnical Society*, vol. 20, no. 8, pp. 55-58, 2005.
- [2] X. P. Ding, Z. M. Qian, S.T. Yang, et al. "A High-Performance Z-Source Inverter Operate with Both Small Inductor and Light-load", in *Proc. of IEEE APEC 2006*, pp. 615-620, 2006.
- [3] Battiston A, Miliami E H, Pierfederici S, et al. "A Novel Quasi-Z-Source Inverter Topology with Special Coupled Inductors for Input Current Ripples Cancellation". *IEEE Transactions on Power Electronic*, vol. 31, no. 3, pp. 2409-2416, 2015.
- [4] G.Joos, J.Espinoza. "Three phase series Var compensation based on a voltage controlled current source inverter with supplemental modulation index control". in *Proc. of IEEE PESC*, pp. 1437-1442, 1994.
- [5] Yushan L., Baoming G., Abu-Rub H, et al. "An Effective Control Method for Quasi-Z-Source Cascade Multilevel Inverter-Based Grid-Tie Single-Phase Photovoltaic Power System". *IEEE Transactions on Industrial Informatics*, vol. 10, no. 1, pp. 399-407, 2014.
- [6] F. Z. Peng. "Z-source inverter". *IEEE Transactions on Industry Application*, vol. 39, no. 2, pp. 504-516, 2003.
- [7] Anderson J, Peng F. Z. "Four quasi-Z-source inverters". in *Proc. of the 39th IEEE Power Electronics Specialist conference*, 2008, pp.2743-2749.
- [8] Y., Xie S. J., C. H. Zhang. "Improved Z-Source Inverter". in *Proc. of the CSEE*, vol. 29, no. 30, pp. 28-34, 2009.
- [9] M. Zhu, K. Yu, F. L. Luo. "Switched Inductor Z-Source Inverter". *IEEE Transactions on Power Electronics*, vol. 25, no. 8, pp. 2150-2158, 2010.
- [10] Amir Hakemi, Majid Sanatkar-Chayjani, Mohammad Monfared. "Δ-Source Impedance Network", *IEEE Transactions on Industrial Electronic*, vol. 64, no. 10, Oct. 2017.
- [11] Siwakoti, Y. P., Town, G. E., Poh Chiang Loh, Blaabjerg, F.. Y-Source inverter. *Power Electronics for Distributed Generation Systems (PEDG)*,

2014 IEEE 5<sup>th</sup> International Symposium on, 2014.

- [12] J. F. Zhang. "Analysis of Influence of Inverter Dead Time on Output Voltage". *Power Electronics*, vol. 41, no. 8, pp. 31-33, 2007.
- [13] Z. L. Cai, T. Hou. "A Novel High Gain Quasi-Z Source Inverter". *Modern Electronic Technology*, vol. 39, no. 24, pp. 149-153, 2016.
- [14] Z. Y. Cheng, H. J. Chen, H. Yu, et al. "Research on Multi-Cascade Switching Inductive Quasi-Z Source Inverter". *Journal of Anhui University (Natural Science)*, vol. 37, no. 6, pp. 48-56, 2013.
- [15] W. Qin, T. Zhang, W. J. Wei, et al. "Direct control strategy for DC link voltage of (quasi) Z-source inverter". *Manufacturing Automation*, vol. 36, no. 3, pp. 118-122, 2014.
- [16] X. P. Fang. Research on Z-source inverter. Hangzhou: Zhejiang University, 2005.
- [17] D. C. Wu, Y. Wu, J. R. Pei, et al. "High-gain Quasi-Z Source Inverter for Boost Unit". *Automation of Electric Power Systems*, vol. 39, no. 21, pp. 138-143, 2015.



**Xupeng Fang** was born in Shandong Province, China, in 1971. He received the B.S. and M.S. degrees from the Shandong University of Science and Technology of China, Qingdao, in 1994 and 1997, respectively, majored in industry automation, electrical drive and its automation, respectively, and the Ph.D. degree from the Zhejiang University of

China, Hangzhou, in 2005, in electrical engineering. He joined the Shandong University of Science and Technology, Qingdao, China, in 1997 and now he is an Associate Professor in the College of Electrical Engineering and Automation. He was a visiting scholar in the Power electronics and Motor drive center of Michigan State University from March, 2013 to March, 2014. He has published over 100 papers, wherein includes over 30 papers in IEEE Transactions and IEEE conference proceedings, and held 16 patents, and has applied for 2 invention patents that in the examination stage. His research interests include Z-source converter and its applications, utility applications of power electronics such as active filters and FACTS devices, renewable resources generation. Dr. Fang is a senior member of China Electrotechnical Society Power Electronics Society and an invited reviewer of IEEE Transactions on Power Electronics, IEEE Transactions on Industrial Electronics, IEEE Transactions on Circuits and Systems, IEEE Transactions on Transportation Electrification and Transactions of China Electrotechnical Society.



**Yingying Tian** was born in Shandong Province, China, in 1994. She received the B.S. from the Ludong University, in 2017, majored in electrical engineering and its automation, and now she is pursuing her Master's degree in the Shandong University of Science and Technology, majored in power system and automation.



**Xiaokang Ding** was born in Shandong Province, China, in 1996. He received the B.S. from the Shandong University of Science and Technology, in 2017, majored in electrical engineering and its automation, and now he is pursuing his Master's degree in the Shandong University of Science and Technology, majored in power electronics and power drive.



**Bolong Ma** was born in Shandong Province, China, in 1984. He received the B.S. degree from the Shengli College of China University of Petroleum, Dongying, in 2015, majored in electrical engineering and its automation, and the Master's degree from the Shandong University of Science and Technology, in 2018, majored in electrical engineering.